Optical Physics of Quantum Wells

David A. B. Miller

Rm. 4B-401, AT&T Bell Laboratories
Holmdel, NJ07733-3030
USA

1 Introduction

Quantum wells are thin layered semiconductor structures in which we can observe and control many quantum mechanical effects. They derive most of their special properties from the quantum confinement of charge carriers (electrons and "holes") in thin layers (e.g 40 atomic layers thick) of one semiconductor "well" material sandwiched between other semiconductor "barrier" layers. They can be made to a high degree of precision by modern epitaxial crystal growth techniques. Many of the physical effects in quantum well structures can be seen at room temperature and can be exploited in real devices. From a scientific point of view, they are also an interesting "laboratory" in which we can explore various quantum mechanical effects, many of which cannot easily be investigated in the usual laboratory setting. For example, we can work with "excitons" as a close quantum mechanical analog for atoms, confining them in distances smaller than their natural size, and applying effectively gigantic electric fields to them, both classes of experiments that are difficult to perform on atoms themselves. We can also carefully tailor "coupled" quantum wells to show quantum mechanical beating phenomena that we can measure and control to a degree that is difficult with molecules.

   In this article, we will introduce quantum wells, and will concentrate on some of the physical effects that are seen in optical experiments. Quantum wells also have many interesting properties for electrical transport, though we will not discuss those here. We will briefly allude to some of the optoelectronic devices, though again we will not treat them in any detail.

2 Introduction to Quantum Wells

First we will introduce quantum wells by discussing their basic physics, their structure, fabrication technologies, and their elementary linear optical properties.

2.1 SEMICONDUCTOR BAND STRUCTURE AND HETEROSTRUCTURES

All of the physics and devices that will be discussed here are based on properties of direct gap semiconductors near the center of the Brillouin zone. For all of the semiconductors of interest here, we are concerned with a single, S-like conduction band, and two P-like valence bands. The valence bands are known as the heavy and light hole bands. Importantly for quantum wells, the electrons in the conduction band, and the (positively charged) "holes" in the valence band behave

as particles with effective masses different from the free electron mass. The simplest "k.p" band theory says that the electron effective mass, m_e, and the light hole effective mass, m_{lh}, are approximately equal and proportional to the band gap energy. For GaAs, which has a band gap energy of ~ 1.5 eV, the actual values are $m_e \sim 0.069\ m_o$ and $m_{lh} \sim 0.09\ m_o$, where m_o is the free electron mass. The heavy hole effective mass, m_{hh}, is typically more comparable to the free electron mass ($m_{hh} \sim 0.35\ m_o$ for the most common situation in quantum wells), and does not vary systematically with the band gap energy.

Quantum wells are one example of heterostructures - structures made by joining different materials, usually in layers, and with the materials joined directly at the atomic level. When two semiconductors are joined, it is not clear in advance how the different bands in the two materials will line up in energy with one another, and their is no accurate predictive theory in practice. Hence, an important experimental quantity is the "band offset ratio"; this is the ratio of the difference in conduction band energies to the difference in valence band energies. For GaAs/AlGaAs heterostructures, for example, approximately 67% of the difference in the band gap energies is in the conduction band offset, and 33% is in the valence band offset, giving a ratio 67:33. In this particular material system, both electrons and holes see higher energies in the AlGaAs than in the GaAs, giving a so-called "Type I" system. Heterostructures in which electrons and holes have their lowest energies in different materials are called "Type II", but such structures will not be considered further here.

Heterostructures in general have many uses. They can be used for advanced electronic devices (e.g., modulation-doped field-effect transistors, heterojunction bipolar transistors, resonant tunneling devices), optical components (e.g., waveguides, mirrors, microresonators), and optoelectronic devices and structures (e.g., laser diodes, photodetectors, quantum well and superlattice optical and optoelectronic devices). Although heterostructures may be useful in electronics, they are crucial in many optoelectronic devices (e.g., lasers). Perhaps their most important technological aspect may be that they can be used for all of these electronic, optical, and optoelectronic purposes, and hence may allow the integration of all of these.

2.2 QUANTUM WELL STRUCTURES AND GROWTH

A quantum well is a particular kind of heterostructure in which one thin "well" layer is surrounded by two "barrier" layers. Both electrons and holes see lower energy in the "well" layer, hence the name (by analogy with a "potential well"). This layer, in which both electrons and holes are confined, is so thin (typically about 100 Å, or about 40 atomic layers) that we cannot neglect the fact that the electron and hole are both waves. In fact, the allowed states in this structure correspond to standing waves in the direction perpendicular to the layers. Because only particular waves are standing waves, the system is quantized, hence the name "quantum well".

There are at least two techniques by which quantum well structures can be grown, molecular beam epitaxy (MBE) (Cho 1991), and metal-organic chemical vapor deposition (MOCVD) (Furuya and Miramoto 1990). Both can achieve a layer thickness control close to about one atomic layer. MBE is essentially a very high vacuum technique in which beams of the constituent atoms or molecules (e.g., Ga, Al, or As) emerge from ovens, land on the surface of a heated substrate, and there grow layers of material. Which material is grown can be controlled by opening and closing shutters in front of the ovens. For example, with a shutter closed in front of the Al oven, but open shutters in from of the Ga and As ovens, GaAs layers will be grown. Opening the Al shutter will then grow the alloy AlGaAs, with the relative proportion of Ga and Al controlled by the temperatures of the ovens. With additional ovens and shutters for the dopant materials, structures of any sequence of GaAs, AlAs, and AlGaAs can be grown with essentially

arbitrary dopings. MOCVD is a gas phase technique at low pressure (e.g., 25 torr). In this case the constituents are passed as gasses (e.g., trimethylgallium and arsine) over a heated substrate, with the resulting composition being controlled by the relative amounts of the appropriate gasses. Hybrid techniques, using the gas sources of MOCVD in a high vacuum molecular beam system, also exist, and are known variously as gas-source MBE or chemical beam epitaxy (CBE) (Tsang 1990). Which technique is best depends on the material system and the desired structure or device. Typical structures grown by these techniques might have total thickness of microns, and could have as many as hundreds of layers in them.

There are many different materials that can be grown by these techniques, and many of these have been used to make quantum well structures. One significant restriction is that it is important to make sure that the lattice constants (essentially, the spacing between the atoms) of the materials to be grown in the heterostructure are very similar. If this is not the case, it will be difficult to retain a well-defined crystal structure throughout the layers - the growth will not be "epitaxial". The growth is simplest when the lattice constants are identical. Fortunately, AlAs and GaAs have almost identical lattice constants, which means that arbitrary structures can be grown with high quality in this materials system. Another commonly used system is InGaAs with InP; in this case, the proportions of In and Ga are adjusted to give a lattice constant for the ternary (three-component) InGaAs alloy that is equal to InP. Use of four component (quaternary) alloys (e.g., InGaAsP) allows sufficient degrees of freedom to adjust both the lattice constant and the bandgap energy. Up to a certain critical thickness, which depends on the degree of lattice constant mismatch, it is possible to grow structures with materials that naturally have different lattice constants. In this case, the materials grow in a highly strained state but can adopt the local lattice constant and retain good epitaxial crystal structure. Such strained materials are of increasing technological importance, although we will not discuss them further here.

A partial list of materials used for quantum well structures includes: III-V's - GaAs/GaAlAs on GaAs (Type I), GaSb/GaAlSb on GaSb (Type I), InGaAs/InAlAs on InP (Type I), InAs/GaSb (Type II), InGaAs/GaAs (Type I, strained); II-VI's - HgCdTe/CdTe, ZnSe/ZnMnSe (semimagnetic), CdZnTe/ZnTe (Type 1, strained); IV-VI's - PbTe/PbSnTe; IV - Si/SiGe (strained).

2.3 PARTICLE-IN-A-BOX QUANTUM WELL PHYSICS

We can understand the basic properties of a quantum well through the simple "particle-in-a-box" model. Here we consider Schrödinger's equation in one dimension for the particle of interest (e.g., electron or hole)

$$\frac{-\hbar^2}{2m}\frac{d^2\phi_n}{dz^2} + V(z)\phi_n = E_n\phi_n$$

(1)

where V(z) is the structural potential (i.e., the "quantum well" potential) seen by the particle along the direction of interest (z), m is the particle's (effective) mass, and E_n and ϕ_n are the eigenenergy and eigenfunction associated with the n'th solution to the equation..

The simplest case is shown in Fig. 1. In this "infinite well" case, we presume for simplicity that the barriers on either side of the quantum well are infinitely high. Then the wavefunction must be zero at the walls of the quantum well.
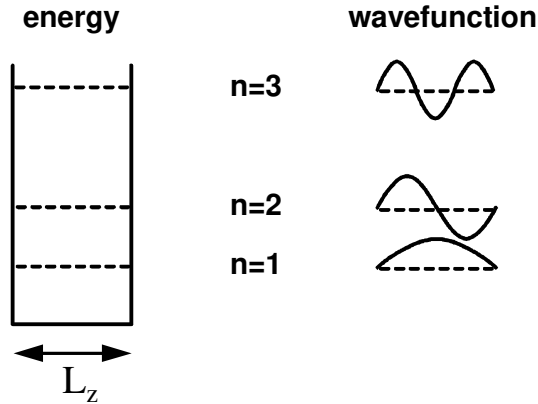
energy   **wavefunction**

n=3

n=2

n=1

L_z

Fig. 1 "Infinite" quantum well and associated wavefunctions.

The solution is then particularly simple:

$$E_n = \frac{-\hbar^2}{2m}\left[\frac{n\pi}{L_z}\right]^2 \quad n = 1, 2, ...\quad \phi_n = A\sin\left(\frac{n\pi z}{L_z}\right)$$

(2)

The energy levels (or "confinement energies") are quadratically spaced, and the wavefunctions are sine waves. In this formula, the energy is referred to the energy of the bottom of the well. Note that the first allowed energy (corresponding to n=1) is above the bottom of the well.

We see that the energy level spacing becomes large for narrow wells (small L_z) and small effective mass m. The actual energy of the first allowed electron energy level in a typical 100 Å GaAs quantum well is about 40 meV, which is close to the value that would be calculated by this simple formula. This scale of energy is easily seen, even at room temperature.
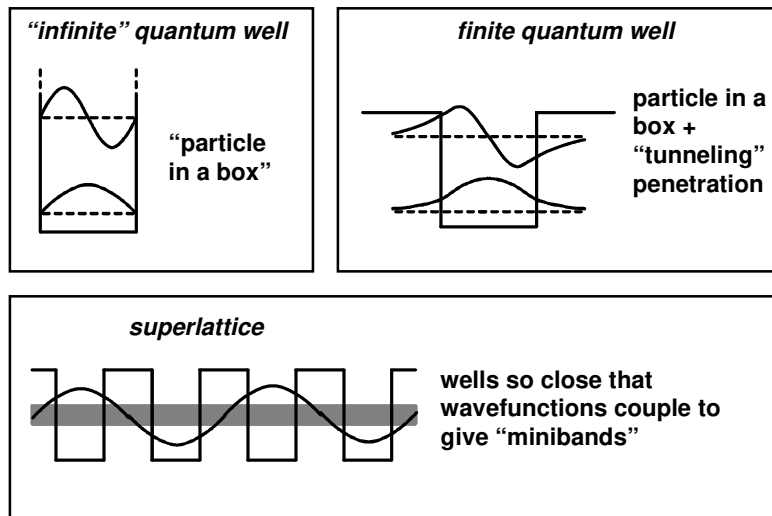

Fig. 2 Comparison of "infinite" quantum well, "finite" quantum well, and superlattice behavior. For the superlattice, a wavefunction for one of the possible superlattice miniband states is shown (actually the state at the top of the miniband).

The solution of the problem of an actual quantum well with finite height of barriers is a straightforward mathematical exercise. It does, however, require that we choose boundary

conditions to match the solutions in the well and the barriers. One boundary condition is obvious, which is that the wavefunction must be continuous. Since the Schrödinger equation is a second order equation, we need a second boundary condition, and it is not actually obvious what it should be. We might think that we would choose continuity of the wavefunction derivative across the boundary; we cannot do so because the masses are different on the two sides of the boundary in general, and it can be shown that such a simple condition does not conserve particle flux across the boundary when the masses are different. One that does conserve particle flux is to choose $(1/m) \, d\phi/dz$ continuous; this is the most commonly used one, and gives answers that agree relatively well with experiment, but there is no fundamental justification for it. This lack of fundamental justification should not worry us too much, because we are dealing anyway with an approximation (the "envelope function" approximation). If we were to use a proper first principles calculation, we would have no problem with boundary conditions on the actual wavefunction.(Burt 1992) The solution of the finite well problem does not exist in closed form (Weisbuch 1987), requiring numerical solution of a simple equation to get the eigenenergies. The wavefunctions of the bound states are again sine waves inside the quantum well, and are exponentially decaying in the barriers. The energies are always somewhat lower than those we would calculate using the infinite well. It can be shown from the solution (Weisbuch 1987) that there is always at least one bound state of a finite quantum well. Fig. 2 illustrates the differences between the idealized "infinite" quantum well, the actual "finite" well.

Also in Fig. 2, we have illustrated a superlattice. It will be useful here to define the difference between quantum wells and superlattices. The simplest, crystallographic, definition of a superlattice is a "lattice of lattices". With that definition, any regular sequence of well and barrier layers would be a superlattice. A more useful definition here is the "electronic" definition; in this definition, we call such a regular structure a superlattice only if there is significant wavefunction penetration between the adjacent wells. Otherwise, the physics of the multiple layer structure is essentially the same as a set of independent wells, and it is more useful to call the structure a multiple quantum well (MQW). If there is significant wavefunction penetration between the wells, we will see phenomena such as "minibands", and the structure is then usefully described as a superlattice. The "minibands" arise when quantum wells are put very close together in a regular way, just as "bands" arise in crystalline materials as atoms are put together. Just as with quantum wells, simple models for superlattices can be constructed using envelope functions and effective masses, and such models are also good first approximations. As a rule of thumb, for well and barrier layers thicker than about 50 Å in the GaAs/AlGaAs system, with a typical Al concentration of about 30 % in the barriers, the structure will probably be best described as a multiple quantum well.

3   Linear Optical Properties of Quantum Wells

To understand the linear interband optical absorption in quantum wells, we will first neglect the so-called "excitonic" effects. This is a useful first model conceptually, and explains some of the key features. For a full understanding, however, it is important to understand the excitonic effects. In contrast to bulk semiconductors, excitonic effects are very clear in quantum wells at room temperature, and have a significant influence on device performance.

3.1 OPTICAL ABSORPTION NEGLECTING EXCITONS

The simplest model for absorption between the valence and conduction bands in a bulk semiconductor is to say that we can raise an electron from the valence band to a state of

essentially the same momentum in the conduction band (a "vertical" transition) by absorbing a photon. The state in the conduction band has to have essentially the same momentum because the photon has essentially no momentum on the scale usually of interest in semiconductors. In this simple model, we also presume that all such transitions have identical strength, although they will have different energies corresponding to the different energies for such vertical transitions. The optical absorption spectrum therefore has a form that follows directly from the density of states in energy, and in bulk (3D) semiconductors the result is an absorption edge that rises as the square root of energy, as shown in Fig. 3.

In quantum wells, for the direction perpendicular to the layers, instead of momentum conservation we have a selection rule. The rule states that (to lowest order) only transitions between states of the same quantum number in the valence and conduction bands are allowed. This rule follows from the fact that the optical absorption strength is proportional to the overlap integral of the conduction and valence (envelope) wave functions. For sinusoidal standing waves, as shown for the infinite quantum well in Fig. 2, there is only a finite overlap between identical standing waves. (This rule is somewhat weaker for finite wells, although it is still a very good starting point.) We can if we wish still view this as conservation of momentum, since we can regard the standing waves as states of specific momenta. (The converse is also true, in that even in bulk semiconductors we can equally well view the momentum conservation rule as following from allowed overlap integrals, in that case between plane wave wavefunctions.)

In a quantum well, the electrons and holes are still free to move in the directions parallel to the layers; hence, we do not really have discrete energy states for electrons and holes in quantum wells; we have instead "subbands" that start at the energies calculated for the confined states. The electron in a given confined state can in addition have any amount of kinetic energy for its in-plane motion in the quantum well, and so can have any energy greater than or equal to the simple confined-state energy for that subband. The density of states for motion in the plane of the quantum well layers turns out to be constant with energy, so the density of states for a given subband really is a "step" that starts at the appropriate confinement energy. Optical transitions must still conserve momentum in this direction, and just as for bulk semiconductors, the optical absorption must still therefore follow the density of states. Hence, in this simple model, the optical absorption in a quantum well is a series of steps, with one step for each quantum number, n. It is easily shown, from the known densities of states, that the corners of the steps "touch" the square root bulk absorption curve (when that curve is scaled to the thickness of this infinite quantum well). Thus, as we imagine increasing the quantum well thickness, we will make a smooth transition to the bulk behavior, with the steps becoming increasingly close until they merge into the continuous absorption edge of the bulk material.
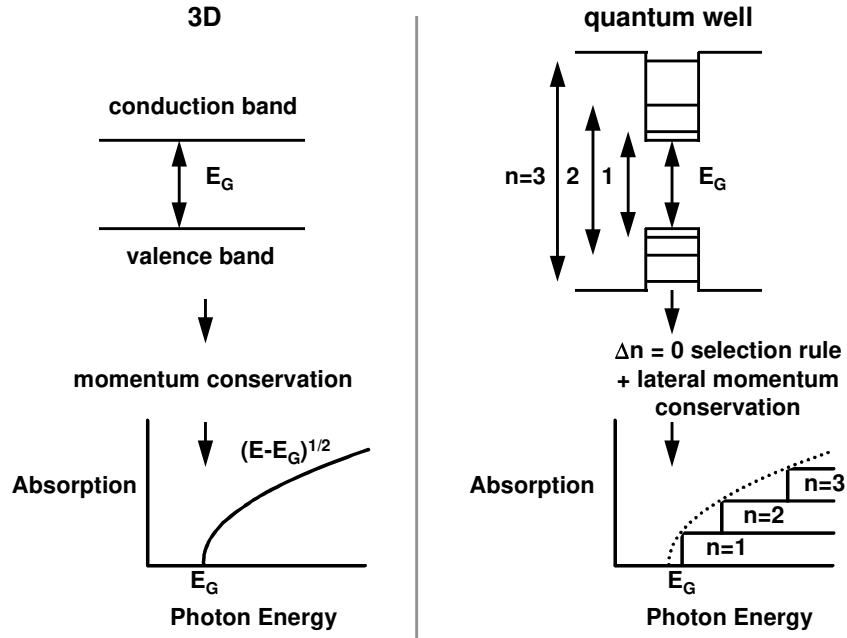
Fig. 3. Optical absorption in bulk (i.e., 3D) semiconductors and in quantum wells, in the simplest model where excitonic effects are neglected.

3.2 CONSEQUENCES OF HEAVY AND LIGHT HOLES

As we mentioned above, there are two kinds of holes that are relevant here, corresponding to the heavy and light hole bands. Since these holes have different masses, there are two sets of hole subbands, with different energy spacings. The light hole subbands, because they have lighter mass, are spaced further apart. The consequence for optical absorption is that there are actually two sets of "steps". The heavy-hole-to-conduction set starts at a slightly lower energy and is more closely spaced than the light-hole-to-conduction set. The heavy hole set is usually dominant when we look at optical absorption for light propagating perpendicular to the quantum well layers.

If, however, we look in a waveguide, with light propagating along the quantum well layers, there are two distinct optical polarization directions: one with the optical electric vector parallel to the quantum well layers (so-called "transverse electric" or TE polarization); and the other with the optical electric vector perpendicular to the quantum well layers (so-called "transverse magnetic" or TM polarization). The TE case is essentially identical to the situation for light propagating perpendicular to the layers, where the optical electric vector is always in the plane of the quantum wells; the optical electric vector is always perpendicular to the direction of propagation for a plane wave. The TM case is substantially different from the TE case, however.

Because of microscopic selection rules associated with the unit cell wavefunctions, for the TM polarization, the heavy-hole-to-conduction transitions are forbidden, and all of the absorption strength goes over to the light-hole-to-conduction transitions. Hence, at least with this simple model, there is now only one set of steps in the absorption. The reason for loss of the heavy hole transitions is not a special property of quantum wells; this kind of selection rule is a consequence of defining a definite symmetry axis in the material, in this case the growth direction of the quantum well layers. Exactly the same selection rule phenomenon will result if

we apply a uniaxial stress to a bulk semiconductor. One practical consequence of this selection rule effect is that quantum well waveguide lasers essentially always run in TE polarization; there are more heavy holes than light holes in thermal equilibrium, and hence the gain associated with heavy holes is larger, and hence the gain is larger for the TE polarization. In general, this simple classification of holes into "heavy" and "light" is only valid near the center of the Brillouin zone. The detailed structure of the valence bands is particularly complicated since the various subbands would actually appear to cross one another. In fact, such crossing are avoided, and the resulting subband structure is quite involved. For many devices, such effects are not very important (at least for a basic understanding of the devices), and we will not discuss such valence band effects further here.

3.3 OPTICAL ABSORPTION INCLUDING EXCITONS

Fig. 4 shows an actual absorption spectrum of a quantum well sample.

We see from Fig. 4 that the quantum well absorption is indeed a series of steps, and simple calculations based on the particle-in-a-box models will correctly give the approximate positions of the steps. But it is also clear that there are sets of peaks in the spectra not predicted or explained by the simple "non-excitonic" model described above. These peaks are quite a strong effect, and will be particularly important near the band-gap energy, here at about 1.46 eV photon energy. Most devices also operate in this region.

To understand these peaks, we need to introduce the concept of excitons. The key point missing in the previous discussion is that we have neglected the fact the electrons and holes are charged particles (negative and positive respectively) that attract each other. Hence, when we have an electron and a hole in a semiconductor, their wavefunctions are not plane waves; plane waves correspond to the case of uniform independent motion of the electron and the hole. Instead, we should expect that the electron and hole wavefunction should correspond to the case where the electron and hole are close to one another because of their Coulomb attraction. The formal error we made in the analysis above is therefore that we did not use the correct eigenfunctions for the electrons and holes, and hence we formally got an incorrect answer when we used those eigenfunctions to calculate the optical absorption.
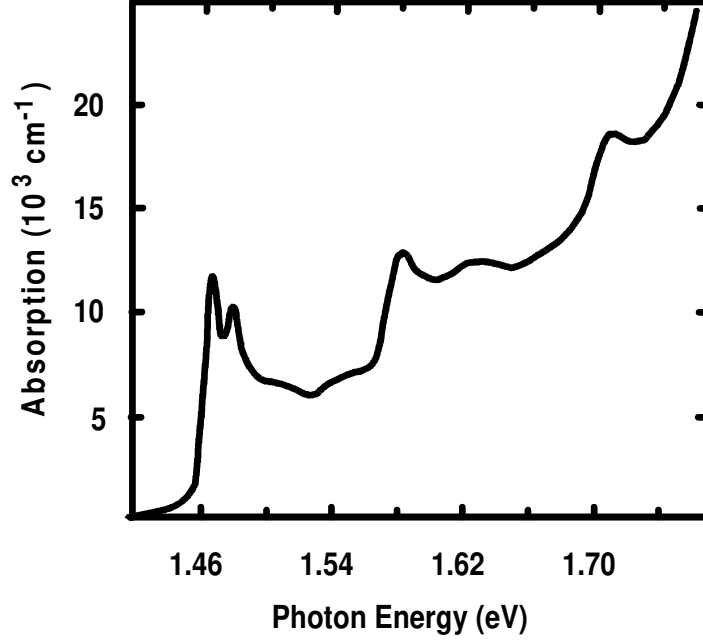
Fig. 4. Absorption spectrum of a typical GaAs/AlGaAs quantum well structure at room temperature.

Unfortunately, to include excitonic effects properly we need to use a different picture, since the whole band structure picture is a single particle picture; it essentially describes the energies seen by either a single electron or a single hole, but cannot handle both at once. Fortunately, there is a simple picture that allows us to understand the resulting excitonic effects.

The correct approach is not to consider raising an electron from the valence band to the conduction band, but rather to consider the creation of an electron-hole pair. In this picture, we find the eigenfunctions of the electron-hole pair in the crystal, and base our calculation of optical absorption on those pair states. First, then, we must understand what are the states of an electron-hole pair in a crystal. Fortunately, at least for the case where the attraction is not too strong, this problem is already solved; it is essentially the same problem as the states of the hydrogen atom, corrected for the different effective masses and dielectric constants in the semiconductor. Using this model, we find, for example, the binding energy of lowest, 1S, exciton is

$$E_B = \frac{\mu e^4}{8 h^2 \varepsilon_R^2 \varepsilon_o^2} \qquad (3)$$

where h is Planck's constant, ε_R is the relative permittivity, ε_o is the permittivity of free space, and μ is the reduced mass

$$\mu = \frac{m_e m_h}{m_e + m_h} \qquad (4)$$

For bulk GaAs (where excitons can be clearly seen at low temperature), $E_B \sim 4$ meV.

Hence, we find the first remarkable property of excitons compared to the non-excitonic model. It is possible to create an exciton with an energy E_B less than that required to create a "free" electron-hole pair. A free electron-hole pair is analogous to an ionized hydrogen atom, and the energy required to create such a free pair in the semiconductor is actually the simple band-gap energy of the single particle picture. Hence we expect some optical absorption at photon

energies just below the band-gap energy. This point is illustrated in Fig. 5, on the left, showing a possible transition at an energy $E_{exciton} = E_{bandgap} - E_B$.

It is not only the absorption that creates the 1S exciton that is important, although under most conditions it is the only one that we see clearly as a distinct peak. In fact the entire absorption spectrum of these kinds of semiconductors is properly described in terms of the complete set of hydrogenic states. For example, the absorption above the band-gap energy results from the creation of excitons in the unbound hydrogenic states. In the classical sense, such states correspond to hyperbolic orbits. There is also additional absorption just below the bandgap energy from the other, bound excitonic states.

Note now that we are explaining the optical absorption in terms of the creation of a particle, the exciton (or, exactly equivalently, an electron-hole pair). It is important to understand that the absorption we see is not that associated with raising an existing hydrogenic particle to an excited state, as would be the case with conventional atomic absorption; we are instead creating the particle. An analogy that may help understand this distinction is the absorption in the vacuum that creates electron-positron pairs. This is illustrated in Fig. 5, on the right.

By absorbing photons in the vacuum, we can in principle create positronium atoms, which are simply hydrogenic systems composed of an electron and a positron (instead of a proton). In this case, we are simultaneously creating a positron in the Fermi sea (the analog of the valence band), as well as an electron. This happens to be a two-photon transition, and is therefore a rather weak effect in practice, but it illustrates the difference between the creation of an atom and the absorption between levels of the atom. A very important difference between these is that in the creation case, we have "excitonic" absorption even when we have no excitons in the material. In the positronium case, it is very clear that there need be no positronium atoms there since we are starting with a perfect vacuum!

In the simple model where we neglected excitonic effects, the strength of a particular transition was determined by the square of the overlap integral between the "initial" (valence subband) state and the "final" (conduction subband) state. In principle, we have a similar result for the present excitonic model, although in this case the initial state is the "empty" crystal, and the final state is the crystal with an exciton added. We will not formally derive the consequences of this change in model, but the net result is that, in the exciton creation case, the strength of the absorption to create an electron-hole pair in a given state is proportional to the probability that the resulting electron and hole will be in the place (strictly, the same unit cell). Now we can understand why the excitonic absorption gives such a strong peak for creation of 1S excitons. In the 1S exciton, the electron and hole are bound closely to one another (within a diameter of about 300 Å in bulk GaAs), and the 1S wavefunction actually peaks at zero relative displacement. Hence the probability of finding the electron and the hole in the same place is actually very large, and so the resulting absorption is strong.
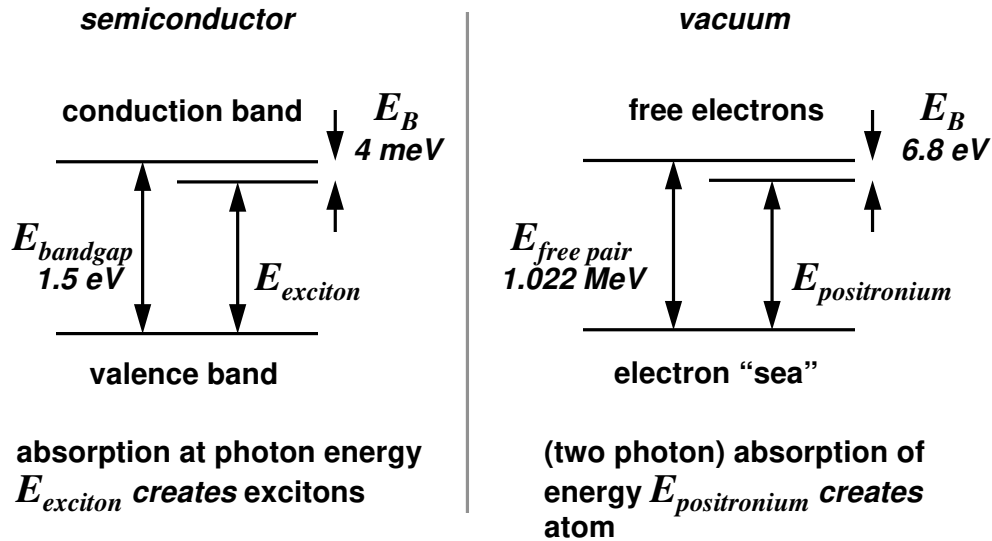
semiconductor | vacuum

conduction band E_B 4 meV

free electrons E_B 6.8 eV

$E_{bandgap}$ 1.5 eV $E_{exciton}$

$E_{free\,pair}$ 1.022 MeV $E_{positronium}$

valence band

electron "sea"

absorption at photon energy $E_{exciton}$ creates excitons

(two photon) absorption of energy $E_{positronium}$ creates atom

Fig. 5. Analogy between excitonic absorption and the optical creation of positronium atoms.

Thus far, we have discussed excitons in general, without explaining why they are particularly important in quantum wells. Excitonic effects are clear in many direct gap semiconductors at low temperature. At room temperature, however, although excitonic effects are still very important in determining the shape and strength of the interband absorption, the actual peaks corresponding to the bound states are difficult to resolve. The main reason for this lack of resolution is that the bound states are rapidly ionized by collisions with optical phonons at room temperature. In fact, they are typically ionized in times short compared with a classical orbit time. By a Heisenberg uncertainty principle argument, the associated optical linewidth is broadened, to such a point that the line is no longer clearly resolvable.

The quantum well offers two important differences compared to the bulk material, both of which stem from the confinement in the quantum well. Fig. 6 shows, in a semiclassical picture, an exciton in bulk GaAs and an exciton in a quantum well.

Hydrogenic theory for the GaAs exciton gives a diameter of about 300 Å, as mentioned above. When we create an exciton in a quantum well that is only 100 Å thick, the exciton must become smaller, at least in the direction perpendicular to the quantum wells. Remarkably, however, it also becomes smaller in the other two directions (in the plane of the quantum well). This surprising conclusion can be checked, for example, by variational calculations. We can rationalize it by saying that nature prefers to keep the exciton more nearly spherical to minimize energy overall. If, for example, we allowed the exciton to become a flat "pancake" shape, it would acquire high kinetic energies from the large second derivatives at the edges of the pancake. It is also the case that the exact solution of the two-dimensional hydrogen atom, corresponding to a very thin quantum well with very high walls, has a diameter one quarter that of the three-dimensional hydrogen atom. The two consequences are: (1) the electron and hole are even closer together than in the three-dimensional case, so the absorption strength to create such an exciton is even larger; (2) the exciton has a larger binding energy because the electron and hole are closer together, and hence it orbits "faster". As a result of the faster orbiting, the exciton is able to complete a classical orbit before being destroyed by the optical phonon, and hence it remains a well-defined resonance. Equivalently, although the linewidth of the quantum well exciton is comparable to that of the bulk exciton, the binding energy is larger, and the peak is

still well resolved from the onset of the "interband" absorption at the band-gap energy. These two reasons explain both why the quantum well excitons are relatively stronger and also better resolved than the bulk excitons. The practical consequence is that in quantum wells we may be able to make some use of the remarkable excitonic peaks since we can see them at room temperature.
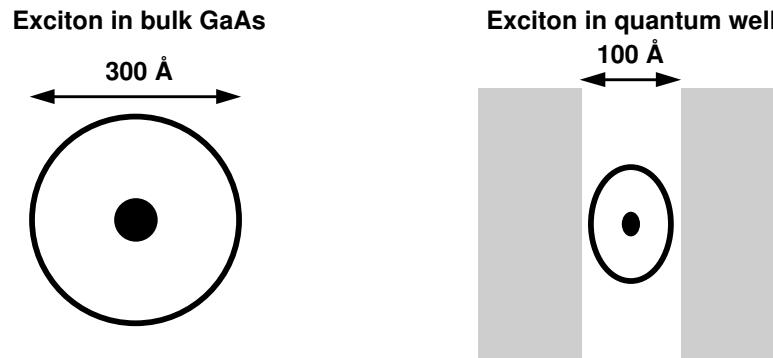
Exciton in bulk GaAs

300 Å

Exciton in quantum well

100 Å

Fig. 6. Comparison of bulk and quantum well exciton sizes and shapes.

Note that in practice we frequently refer to the peaks in the spectrum as the exciton peaks or the exciton absorption peaks. It is important to remember always that these peaks represent the absorption that *creates* the (1S) exciton, and also that all of the rest of the interband absorption is also excitonic, although not to create the 1S state. Loosely, we often talk of "the exciton" as meaning only the 1S exciton.

Incidentally, the two strong peaks that we typically see near the band-gap energy are the 1S exciton absorption peaks associated with the first heavy-hole-to-conduction transition (the stronger peak at lower photon energy) and with the first light-hole-to-conduction transition (the weaker peak at slightly higher photon energy).

4.   Nonlinear Optics in Quantum Wells

There are many possible nonlinear optical effects in quantum wells. Here we will discuss only one class of effects, namely those related to optical absorption saturation near to the band-gap energy. This particular set of effects has been strongly considered for various different kinds of devices, and is a serious candidate for applications in laser modelocking.

In the simplest case, we shine a laser beam on the material so that the resulting optical absorption generates a significant population of electrons and holes, either creating "excitons" (i.e., electron-hole pairs initially in bound hydrogenic states) or "free carriers" (i.e., electron-hole pairs initially in unbound hydrogenic states). Absorbing directly into the exciton (absorption) peaks will generate excitons, whereas absorbing at higher photon energies will generate free carriers. For steady state effects at room temperature with continuous laser beams, it makes little difference which we generate, since the excitons will ionize rapidly (e.g., in ~ 300 fs) and in thermal equilibrium we will essentially have only free carriers anyway. Fig. 7 shows the effect on the absorption spectrum of generating a significant density (e.g., ~ 10^{17} cm^{-3} free carrier density) in the quantum wells.
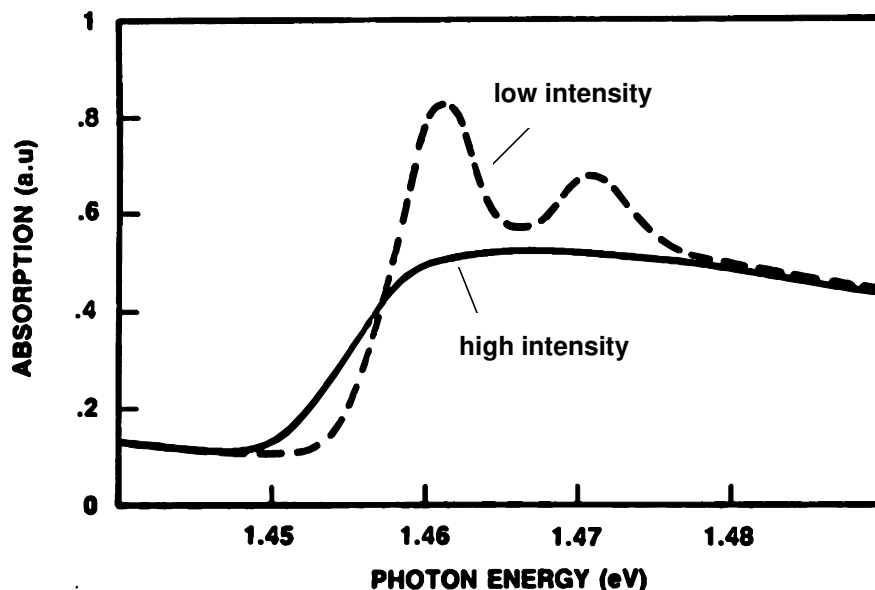
Fig. 7. Absorption spectrum without (dashed line) and with (solid line) optically created free carriers.

As can be seen from Fig. 7, with the presence of such a free carrier density, the exciton peaks have become saturated. The detailed physics of such phenomena is very complicated, and can only be analyzed using many-body theory. We can, however, understand qualitatively various of the mechanisms (Chemla et al. 1984) (Schmitt-Rink et al. 1985). It is important in understanding these mechanisms to remember that the excitonic absorption peaks are associated with the *creation* of excitons. The simple absorption saturation mechanism that we would see in, for example, an atomic vapor, in which the absorption saturates when half of the atoms have been excited to their upper state, does not exist here; there is no density of atoms to start with since there are no excitons present and hence we cannot deduce any density of excited atoms at which saturation occurs by such an argument.

There is, however, one mechanism that is particularly easy to understand. Our physical intuition tells us that we cannot create two similar excitons in the same place; this is exactly like trying to create two atoms in the same place. Hence, as we begin to fill up space with excitons, we will start to run out of space to create more. Consequently, the probability of being able to create more excitons must reduce, and so the optical absorption associated with creating them must decrease. Therefore the exciton absorption line will saturate. This mechanism is illustrated on the left of Fig. 8. For such a mechanism, we will get saturation with about one created exciton per exciton area, which works out to an exciton density of about 10^{17} cm^{-3}.

The real reason for this saturation mechanism is Pauli exclusion; we cannot have two electrons in the same state in the same place. It is also true that free carriers, if they are "cold" enough to be in the states near the band center from which the exciton is comprised, can also prevent creation of more excitons, again by the Pauli exclusion principle. This is illustrated on the right of Fig. 8.
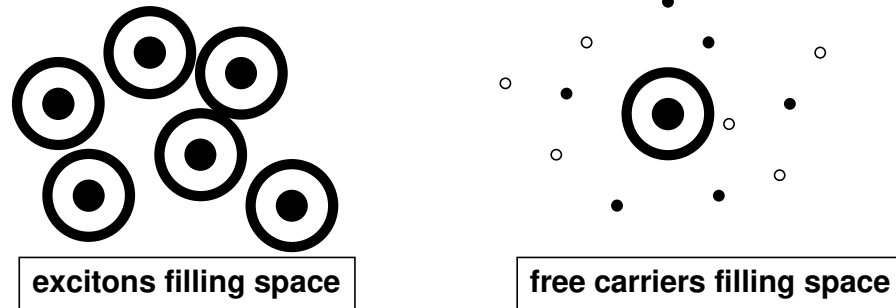
Fig. 8. Illustration of saturation by filling space with excitons (left) and filling space with free carriers. At a density of one exciton per exciton volume, or one "cold" free carrier per exciton volume, it becomes essentially impossible to create any more excitons. This can be visualized geometrically in terms of the probability of trying to "throw" one more exciton onto the plane without it landing on any of the other excitons or free carriers.

Although we have discussed the saturation mechanisms so far in a qualitative and simplistic way, it turns out that these mechanisms are rigorously correct, with the only detail being the effective area of the exciton to use in the argument (Schmitt-Rink et al. 1985). There are also other mechanisms that are somewhat less obvious, and some of these are of comparable size (Schmitt-Rink et al. 1985). A second class of mechanisms that will change the absorption is screening effects. If we create a density of free carriers, they will tend to change the dielectric constant, and hence change the size of the exciton, typically increasing it. If the size of the exciton increases, then the probability of finding the electron and hole in the same place decreases; hence the optical absorption strength decreases, giving an effect that also behaves like saturation. This direct, classical Coulomb screening is thought to be weak in quantum wells because the walls of the wells prevent the movement of charge necessary for effective screening. There is, however, an even more subtle effect that is actually of comparable size to the other "saturation" mechanisms, which is exchange screening. Essentially, when we include the effect of Pauli exclusion in our calculations, we find that the results we would calculate using our simple classical Coulomb effects are not correct at high density, because the Pauli exclusion forces the electrons to be further apart than we had thought (and similarly for the holes). This is described as if it were a screening effect, although it is actually a Pauli exclusion effect that causes us to correct our previous Coulomb calculation. This exchange screening also tends to increase the size of the exciton, reducing absorption.

Although in the steady state at room temperature, we see primarily the effect of free carriers on excitons, at lower temperatures or at short time scales we can see the effect of excitons on excitons. These latter effects are actually typically somewhat stronger (e.g., a factor of 1.5 - 2). Hence, if we initially create excitons and monitor the saturation of the exciton peaks, we can see a fast transient absorption saturation associated with the exciton-exciton effects, followed by a somewhat weaker saturation as the excitons ionize. This actually allows us to measure the exciton ionization time, which is about 300 fs at room temperature.

These saturation effects associated with the exciton peak in quantum wells are relatively sensitive. They have been explored for a variety of nonlinear optical switching devices. Even with the additional benefits of the strong quantum well excitons, these effects are not large enough to make low enough energy devices for current practical systems interest for information processing. The effects are important, however, for two reasons. One reason is that they set limits on the operating power of other devices, such as the modulators and electroabsorptive switches discussed briefly below. Secondly, the effects are large enough for serious use as mode

locking saturable absorber elements for lasers, and this is becoming practical now (Smith et al. 1985) (Keller et al. 1991) (Chen et al. 1991) .

5. Quantum Well Electroabsorption Physics

When electric fields are applied to quantum wells, their optical absorption spectrum near to the band-gap energy can be changed substantially (Miller et al. 1985a), an effect we can call electroabsorption. Such effects have been extensively investigated for optical modulators and switches. There are two very distinct directions in which we can apply electric fields to quantum wells, either with the electric fields parallel to the layers or with the electric field perpendicular to the layers. The case of fields perpendicular to the layers is the one most peculiar to quantum wells, and it is called the Quantum-Confined Stark Effect (QCSE). Here, we will first discuss the case of fields parallel to the layers.

5.1 ELECTRIC FIELDS PARALLEL TO THE LAYERS

For the case of electric fields parallel to the layers, we get effects that are qualitatively similar to those seen in bulk semiconductors. The benefit of the quantum well here is that we can exploit the excitonic electroabsorptive effects at room temperature. The main effect we see is that the exciton absorption peak broadens with field.
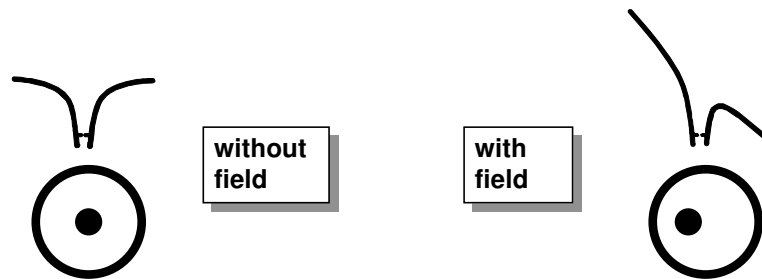

Fig. 9. Effect of field on quantum well excitons for fields parallel to the layers.

Fig. 9 illustrates qualitatively the Coulomb potential of the electron in the presence of the hole, and sketches how the exciton is deformed as the field is applied. In principle, when we apply an electric field to a hydrogenic system, we can shift the energy levels and the resulting transition energies, an effect known in atoms as the Stark effect. For a symmetrical state, such as the ground state of a hydrogenic system, the Stark effect can be viewed as the change in electrostatic energy caused by polarizing the atom with the field, **E**. The change in energy is therefore - (1/2) **P.E**, where **P** is the induced polarization. This corresponds to a reduction in the energy of the hydrogenic system. Hence, we might expect that as we apply an electric field to a semiconductor, we should see the 1S exciton absorption peak move to lower energies, because the energy of the resulting exciton we create is lower by this Stark shift.

It is true that there is such a Stark shift, but it is not the dominant effect that we see. The reason is that the Stark shift of a hydrogenic system is limited to about 10% of the binding energy. Since the binding energy of the exciton is only about 10 meV, the shift is therefore limited to about 1 meV, and hence it is not a very large effect. When we try to shift the energy by more than this, the hydrogenic system becomes field ionized (i.e., the electron and hole are "ripped" apart by the field) so rapidly that the particle cannot complete even a substantial fraction of a classical orbit before being destroyed, and the whole concept of a bound state loses

any useful meaning. In fact, what we see primarily as we apply the field is the broadening of the exciton absorption resonance caused by the shortening of the exciton's lifetime - again, a "Heisenberg uncertainty principle" broadening. (It is just possible to see the shift at low fields in a carefully controlled experiment.)
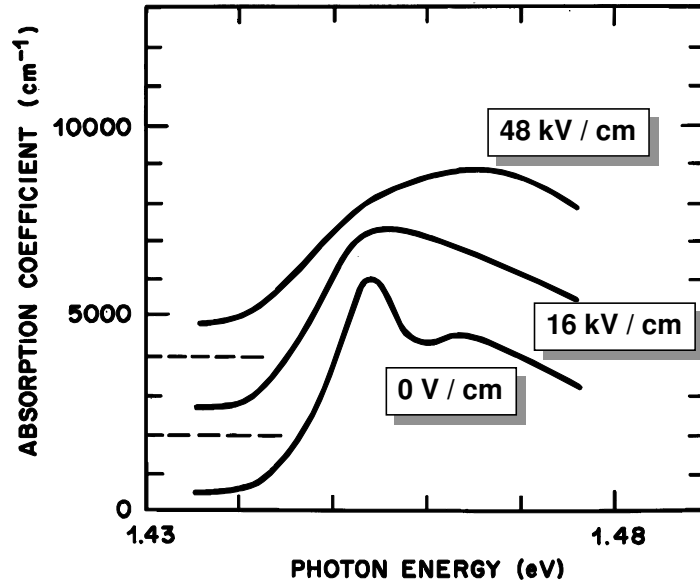
Fig. 10. Absorption spectra for a quantum well sample at room temperature with various electric fields applied in the plane of the quantum well layers. The spectra are shifted vertically for clarity. The exciton peaks broaden with field.

It is worth noting that the fields we are capable of applying to the exciton are gigantic in a relative sense. Applying 1V / μm (= 10^4 / cm) corresponds to a field of one binding energy (~ 10 meV) over one exciton diameter (~ 100 Å). Such a field corresponds to a massive perturbation, certainly much larger than can readily be achieved with a hydrogen atom itself. It is also not surprising that such a field should cause the exciton to be field-ionized in less than a classical orbit time.

Fig. 10 shows a typical set of spectra for parallel field electroabsorption in quantum wells. The broadening and disappearance of the peaks is clearly seen. One consequence is the appearance of a weak absorption tail at lower photon energies. The appearance of this tail is often referred to as the Franz-Keldysh effect. This is somewhat misleading, however, since the Franz-Keldysh effect is really a non-excitonic effect, whereas excitonic effects dominate near to the band-gap energy; the Franz-Keldysh effect, for example, cannot model the exciton broadening at all.

5.2 ELECTRIC FIELDS PERPENDICULAR TO THE LAYERS

The behavior of the electroabsorption for electric fields perpendicular to the quantum well layers is quite distinct from that in bulk semiconductors. Fig. 11 shows a typical set of spectra.
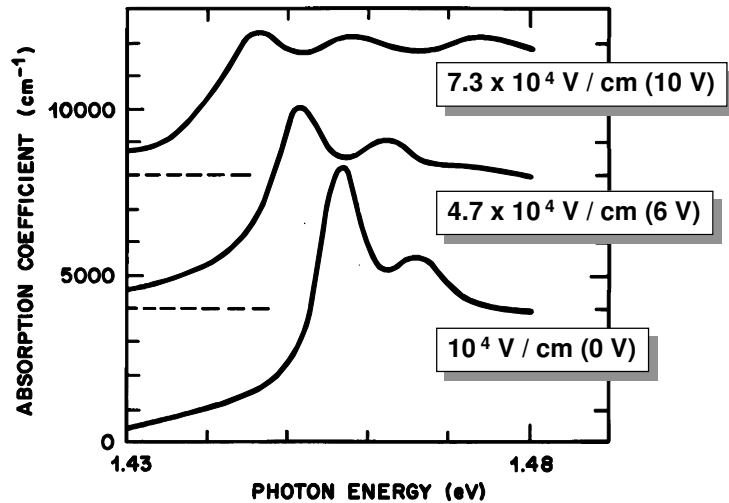
Fig. 11. Absorption spectra for electric fields applied perpendicular to the quantum well layers. The spectra are shifted vertically for clarity. The voltages correspond to those applied to a diode structure containing quantum wells.

Here we can see that, instead of being broadened by the electric field, the exciton absorption peaks are strongly shifted by the field. The shifts can be 10's of meV, and the applied fields here can be much larger than those shown above for the parallel field case, while still preserving the exciton peaks.

The reason for the difference in the electroabsorption in the perpendicular field case is a straightforward consequence of the quantum well. As we apply an electric field perpendicular to the layers, we pull the electron in an exciton in one direction (towards the positive electrode) and the hole in the other direction, just as we would expect. The difference is that the walls of the wells prevent the exciton from field ionizing. Instead, the electron becomes squashed against one wall of the quantum well and the hole against the other, as illustrated in Fig. 12 for the lowest electron and hole states (n=1). Because the electron and hole are still relatively close to one another, they are still strongly attracted by their Coulomb attraction, and they still orbit round one another in the plane of the quantum wells, albeit in a somewhat displaced orbit. Hence the exciton can still exist as a particle for times longer than a classical orbit time, and the exciton absorption peak is not greatly broadened. Because the particle still exists even with very strong fields, we can obtain very large Stark shifts. In fact, the Stark shifts can be many times the binding energy (this is not unphysical since we are decreasing the energy, not increasing it). To see this effect, it is of course important that the quantum well is significantly smaller than the bulk exciton diameter; otherwise, the exciton can effectively be field-ionized simply by separating them by a sufficient distance within the well. For obvious reasons, this shift of the exciton absorption peaks is called the Quantum-Confined Stark Effect (QCSE). In principle, we could see similar effects with a hydrogen atom itself, but to do so we would need to confine the hydrogen atom within a distance less than 1 Å, and apply fields of ~ 10^{11} V/cm, both of which are currently impractical.
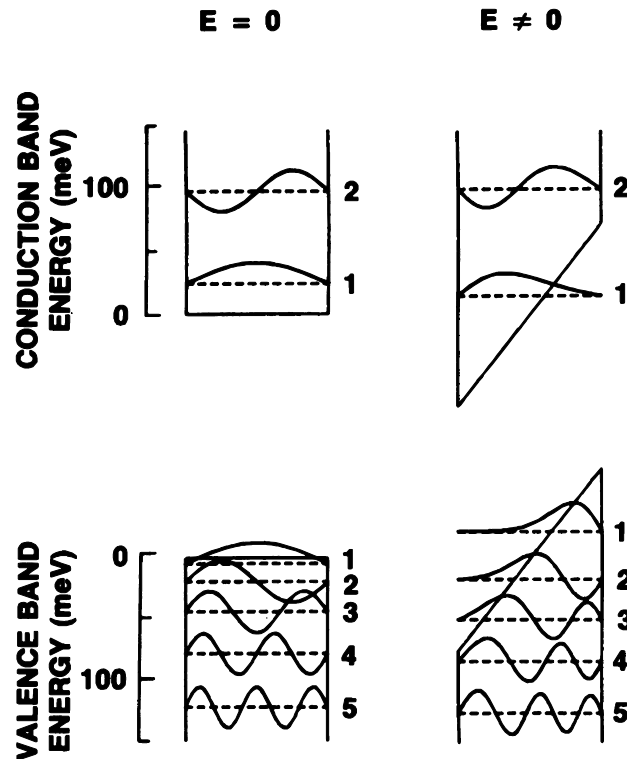
Fig. 12. Electron and hole wavefunctions for the first few states in an "infinite" quantum well. Without field, the wavefunctions are sinusoidal; with field they are Airy functions.

We can also see from Fig. 11 that, as the exciton absorption peaks are shifted to lower energies, they do become weaker. The reason for this is that the electron and hole are being separated from one another by being pulled in opposite directions, and hence there is less probability of finding them in the same place. Consequently, the absorption strength decreases. It is worth mentioning here that, as absorption strength is lost in this way by the so-called "allowed" transitions (e.g., the first hole state to the first electron state), it is picked up by formerly "forbidden" transitions (e.g., the second hole state to the first electron state) (Miller et al. 1986). With the applied field, the electron and hole wavefunctions in all of the levels are distorted; instead of being sinusoidal, they are Airy functions, as illustrated in Fig. 12. In this case there tend to be finite overlap integrals between all possible states. The strengths of these various "forbidden" transitions are bounded by sum rules - essentially, the electric field cannot change the total amount of absorption in the system.

We will not give details of the quantum mechanical calculation of the shifts of the peaks. It is, however, relatively straightforward. Although the above explanations for the reasons for the continued existence of the excitons are important for the effect, and the excitonic effects are also important for the strength of the absorption, the dominant part of the shift comes from the underlying shift of the single particle states. We can see this shift in Fig. 12, where we see the n=1 electron level moving down and the n=1 hole level moving up; the net result is that the energy separation between the n=1 hole and electron levels is reduced with field. The shift in the exciton binding energy itself is relatively unimportant by comparison (typically a few meV). The calculation of the shift of individual electron or hole levels with field can be done by various means. For a tilted well, the wave equation becomes Airy's differential equation, and hence the exact solutions (e.g., as in Fig. 12) are Airy functions.

It is also, incidentally, quite correct to view the quantum-confined Stark effect shifts as resulting from the polarization of the exciton by the electric field, hence giving a (1/2) **P.E** shift in the exciton energy. To lowest order, the polarization is proportional to the field (i.e., the induced separation of the electron and hole is initially linear with field), and so the QCSE is a quadratic effect to lowest order.

Although we have discussed effects here only for the case of simple "rectangular" quantum wells, many other forms of quantum wells are also possible, such as coupled quantum wells, graded quantum wells, stepped quantum wells. These other structures also show related effects induced by applied electric fields, although we will not discuss these here. Also, superlattices show a class of effects induced by fields, known as Wannier-Stark localization. This effect and effects in coupled quantum wells are closely related.

5.3 QUANTUM WELL ELECTRO-OPTIC DEVICES

The QCSE is particularly attractive for optical modulators. A simple device structure is shown in Fig. 13. A quantum well region, typically containing 50 to 100 quantum wells, is grown as the undoped "intrinsic" ("i") region in a p-i-n diode. This quantum well region will therefore have a thickness of about 1 - 2 microns. In operation, the diode is reverse biased. 1 V across 1 micron corresponds to a field of 10^4 V/cm, so substantial QCSE shifts and changes in the absorption spectrum can be made with applied voltages of the order of 5 - 10 V. The reverse biased diode is convenient because there is no conduction current that needs to flow in the diode in order to apply these relatively substantial fields.

The "p" and "n" regions of the diode are made out of a material that is substantially transparent at the wavelength of interest. In the case of GaAs quantum wells, they would most likely be made out of AlGaAs, the same material as used for the quantum well barriers. For the particular case of GaAs/AlGaAs quantum wells, the usual substrate material is GaAs. Unfortunately, GaAs is opaque at the wavelengths used with such modulators, hence the substrate has to be removed for a transmissive modulator, such as the one in Fig. 13.

There are two very important features of the quantum well modulator. The first is that the electroabsorptive mechanisms (the QCSE) in the quantum well are strong enough to make a modulator that can work for light propagating *perpendicular* to the surface of the semiconductor. Despite the fact that this modulator will typically only be a few microns in thickness altogether, it can make changes in transmission of a factor of 2 - 3 in a single pass of a light beam. This modulation is large enough to make usable systems. This feature has the very important consequence that one can therefore make two-dimensional arrays of devices. This opens up many possibilities for novel highly-parallel optoelectronic systems.
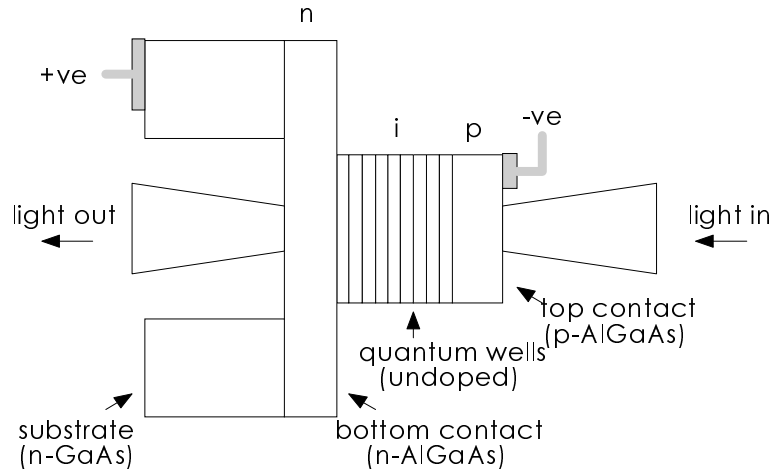
Fig. 13. Quantum well modulator diode structure.

A second key feature is that the operating energy of this modulator is small. The amount of energy required to change the optical properties in this modulator is essentially the stored electrostatic energy at the operating field. In other words, one has to charge up the capacitance of the device. The capacitance of a 1 micron square area of a semiconductor device 1 micron thick is approximately 10^{-16} F. Hence the total energy required to charge the device is (1/2) CV^2 ~ 1 - 2 fJ/μm^2. This energy density is comparable to the energy density in switching electronic devices, and is much smaller (e.g., by a factor of ~ 100) than the energy per unit optical area required to turn on a laser diode or saturate an optical absorption. Hence this device is very attractive as a potentially highly efficient optical output device for electronic circuits.

In addition, the speed limit on the use of the QCSE is probably in the range of ~ 100 fs or less. Practical modulator devices will not be limited by the electroabsorption mechanism itself, seeing instead only the usual resistive/capacitive limits in applying voltage to the diodes. Because the diodes can be small, the capacitance can also be small, and hence these devices are attractive for high speed modulators.

The QCSE can also be used effectively for waveguide modulators (where the light propagates along the surface). In this case, a useful modulator can be made with only a few quantum wells because the propagation distance can be long (e.g., 100 microns). As a result, waveguide quantum well modulators can operate with low voltages (e.g., < 1 V). The change in absorption from the QCSE also results in changes in refractive index (through the Kramers-Krönig relations), and waveguide refractive modulators can also be made.

The Self Electrooptic Effect Device (SEED) principle is to combine a quantum well modulator (or a set of modulators) with a photodetector (or a set of photodetectors) to make an optically controlled device with an optical output (or outputs) (Miller et al. 1985b) (Miller 1990c). A major reason for thinking about such a class of devices is an opportunity for efficient integration. Quantum well modulators driven directly by external electrical connections are limited in speed and operating energy by the external electrical parasitics, such as capacitance and the need to drive with impedance matched lines at high speeds. The modulators themselves can be driven with very low total energies if the drive is electrically local and not brought in by some external connection. Furthermore, since they are semiconductor devices, the prospects for integration with various optoelectronic and electronic devices are good.

Although it is often the case that the conversion from optics to electronics and back to optics is inefficient and costly, this need not be the case if the devices are well integrated. In practice,

the quantum well devices can be integrated effectively, and allow two-dimensional arrays of smart optoelectronic units or "smart pixels". Such devices offer new possibilities in information processing and switching architectures.
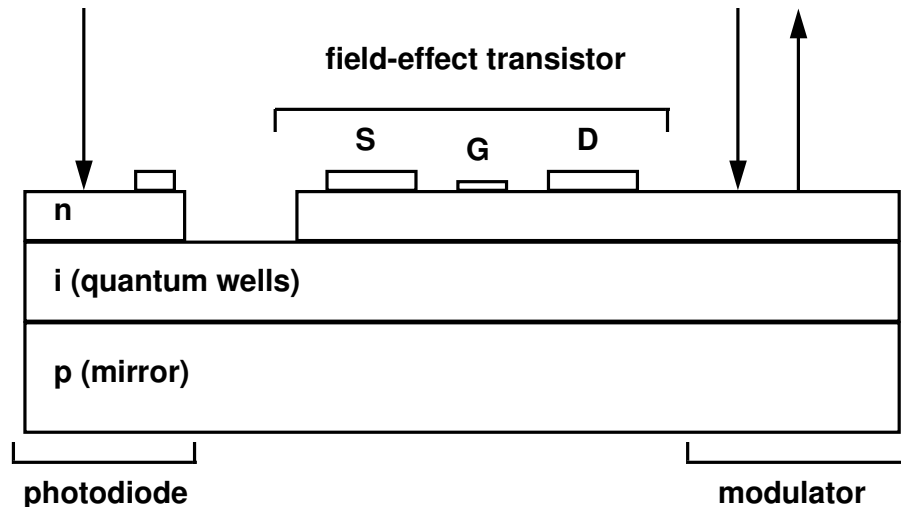

Fig. 14. Concept of the field-effect transistor SEED (FET-SEED). S - source; G - gate; D - drain.

Various optical switching and linear analog devices are possible using combinations of quantum well diodes, without any transistors. These rely on positive or negative feedback; the generated photocurrent leads to a change in voltage across the quantum well diodes, which in turn changes the optical absorption and hence the photocurrent. The feedback can be positive or negative depending on whether the absorption decreases or increases with voltage respectively. Positive feedback can lead to bistable switching. The best-known such device is the symmetric-SEED, which consists of two quantum well diodes reverse-biased in series; this "S-SEED" shows various digital (Lentine et al. 1989) and analog (Miller 1993) (de Souza 1993) modes.

Quantum well diodes, operating as both photodetectors and modulators, can also be integrated with transistors. There are at least two reasons to do such integration. First, using transistors for electronic gain allows the optical energy requirements to be reduced. A second reason is that electronics is very good at performing complex logic functions, at least locally. Combining electronics with the abilities of optics for interconnection may allow the best of both worlds. Indeed there are many advantages of optics for interconnection that become apparent once a good integration technology is available (Miller 1989).

Fig. 14 shows the concept of one integration, the field-effect transistor SEED (FET-SEED) (Miller et al. 1989) (D'Asaro et al. 1993). Here a quantum well diode is grown on top of a mirror as usual, in this case with the n-layer at the top. Then field effect transistors can be fabricated in the top layer. Hence this concept allows photodetectors for optical inputs, transistors for gain and logic, and quantum well modulators for optical outputs.

The present state of the art in this technology is that, in the laboratory, small circuits have been operated with 22 fJ input optical energy, and at speeds up to 650 Mb/s. In actual multistage systems, larger "smart pixels" are operating with 100 fJ optical input energy at 155 Mb/s. A smart pixel array with 96 optical beams and 400 transistors was used in this system (Lentine et

al. 1993). Such operating energies and speeds are of serious interest. For example, with 100 fJ input energy and a factor of 10 loss overall in an optical system, a 1 W laser has sufficient power to drive 1 Tb/s of information through a system. This is a very large data rate, and one that is difficult to achieve with purely electronic systems for a number of reasons (mostly related fundamentally to the skin effect and Maxwell's equations).

Another approach to such integration is to combine quantum well devices with silicon electronics. There has been success in monolithic integration of quantum well diodes onto silicon (Goossen et al. 1989), and it seems likely that various other hybrid schemes might also be possible (Goossen et al. 1993).

6. Terahertz Oscillations in Coupled Quantum Wells

One area of current interest in optical physics of quantum wells is in measuring coherent quantum processes. A particular example of this is recent work on terahertz oscillations excited by short optical pulses. In this work, we can create a quantum mechanical system in a particular linear superposition of states, including setting the quantum mechanical phases in the superposition. We can then watch the system evolve in time, and, importantly, we can measure the evolution of the system with a time resolution short compared to the time scale of the evolution.

One appropriate system for this work is a "coupled" quantum well pair. It is well known, and easy to show, that a pair of quantum wells separated by a thin barrier will have two coupled states. The lower energy state of the pair has a symmetric combination of the two individual well states, and the higher energy state of the pair has an antisymmetric combination. The splitting, ΔE, between these two states becomes larger as we reduce the thickness of the barrier, and can readily be made of the order of 5 - 10 meV in actual coupled wells. If we were to prepare this system so that there was one "electron" in one of these wells initially, it would oscillate back and forward between the two wells with a frequency $\nu = \Delta E / h$. For ΔE's of 5 - 10 meV, the corresponding frequencies are about 1.2 - 2.4 THz. The system oscillates because it is not in an eigenstate, but is rather in the linear superposition of two eigenstates.

Because the electron is moving back and forth between the two wells, there is actually a current in this system at these frequencies (or equivalently an oscillating polarization). As a result, this system will actually emit electromagnetic radiation in the terahertz region. If we can detect the electric field of the terahertz radiation (rather than merely its intensity), we will be able to measure the time evolution of this oscillating polarization, including both amplitude and phase. Hence we can monitor the evolution of the phase of the quantum mechanical system, a rather unusual ability.

WW NW

THz signal

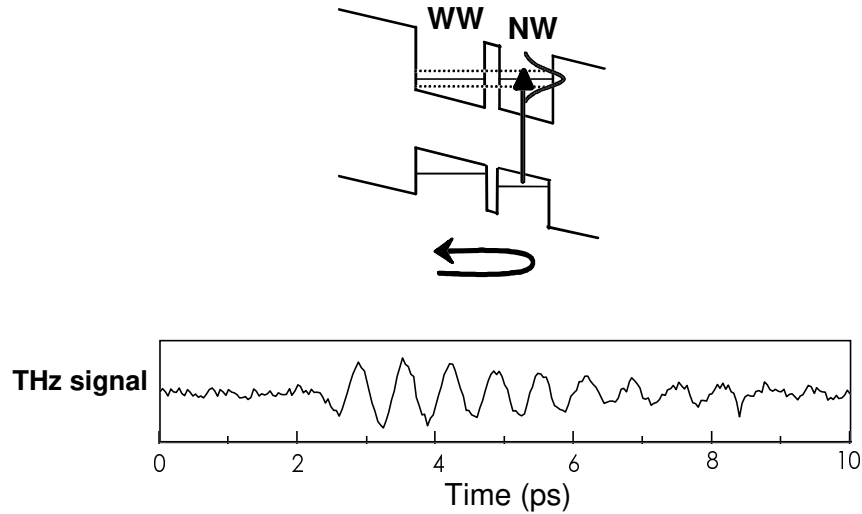0   2   4   6   8   10

Time (ps)

Fig. 15 Schematic diagram of a biased coupled quantum well (upper part of the figure) with both coupled states excited simultaneously by an appropriate short (and hence broadband) optical pulse, resulting in oscillation as shown by the resulting detected terahertz oscillation (lower part of the figure). This particular structure has a narrow well (NW) and a wide well (WW).

The actual sample structure for this experiment and a resulting terahertz signal are shown in Fig. 15. We excite the system with a short optical pulse whose frequency bandwidth covers both of the coupled states so that we excite a linear superposition of them. Note that the short optical pulse is essentially fully coherent - the frequency spectrum is not simply like a small slice out of the spectrum from a light bulb, but has a definite phase relation between the different frequency components; as a result, the two states are excited with a definite phase relation (actually the phase relation that puts the electrons initially in the right hand well. In this particular structure we have used an experimental trick. The two wells are not identical, though we have applied an electric field to "line up" the lowest states in the two wells so we still have coupled wells. The reason for the asymmetry is so that the optical excitation only creates electrons in the right hand well. (In a symmetric structure, equal populations would be created in both wells, and there would be no net oscillation.) The terahertz signal starts after the creation of the electrons in the right hand well, and shows the expected oscillation. The oscillation decays in time, in this case because of dephasing of the excitation from collisions with phonons, other particles, or imperfections.
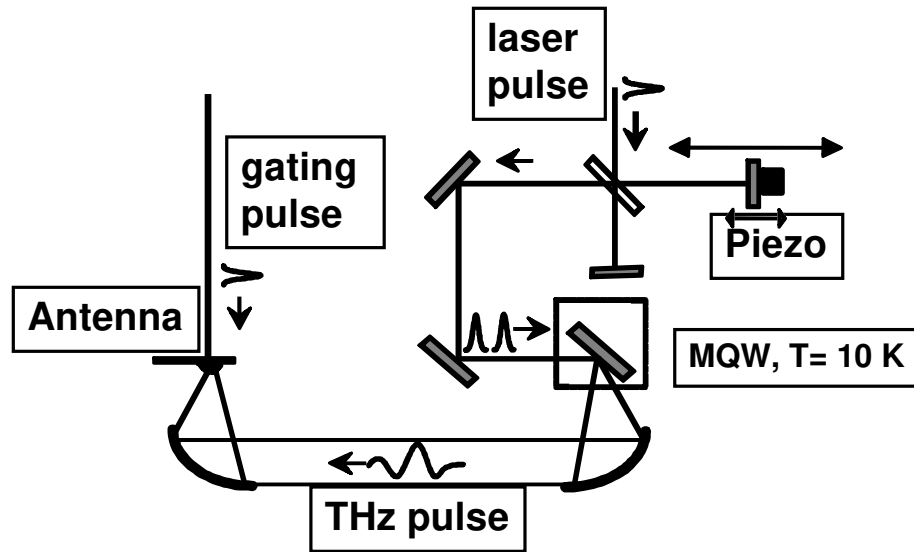
Fig. 16 Experimental setup for two pulse excitation of a quantum well sample with controlled phase between pulses, and subsequent measurement of the resulting terahertz electric field pulse by gated photoconductive sampling of a receiving antenna.

The experimental apparatus to perform these experiments is shown in Fig. 16. This apparatus is also capable of generating two optical pulses from the original laser pulse with a controllable delay set by the piezo translation stage. The excitation pulse (or pulses) are incident on a multiple (coupled) quantum well sample in a cryostat. As a result of this excitation, the sample emits some terahertz electromagnetic radiation. This radiation is collimated by a parabolic mirror, sent to another parabolic mirror and focussed onto an antenna. The antenna is a classical dipole antenna. The instantaneous voltage from the antenna is sampled by a photoconductive sampling gate. This gate "opens" for a short time after it is hit with a short optical gating pulse. The resulting charge that flows through the gate to a conventional electrical signal detection system is therefore proportional to the instantaneous terahertz electric field. The entire terahertz signal is traced out by repeating the experiment for progressively longer delays between the exciting laser pulse and the gating pulse. Such delays are controlled by simple linear translation of a mirror.

This apparatus also illustrates that such terahertz experiments lie in an overlap region between various different regimes. The terahertz signal is generated quantum mechanically, focussed optically and detected like a radio signal. The photon energy or frequencies involved are such that we can move between optics and radio techniques, and between quantum mechanical and classical descriptions. It is also true that in this regime we are at the boundary between classical electrical transport and coherent transport; the coupled well oscillation can be viewed as a coherent transport phenomenon, and it is also possible to observe normal classical transport on these time-scales. Finally, it is possible to view the terahertz generation as a second order nonlinear optical process - technically a difference frequency generaion, and so we are also at the boundary between coherent transport and nonlinear optics.

When we extend these experiments to excitation by two closely spaced optical pulses, we get into a regime that exposes much more of the quantum mechanical nature of this process, and which at first sight is counter-intuitive. Fig. 17 shows the resulting signals for excitation by two pulses when the time separation of the two pulses corresponds to two complete oscillation periods.
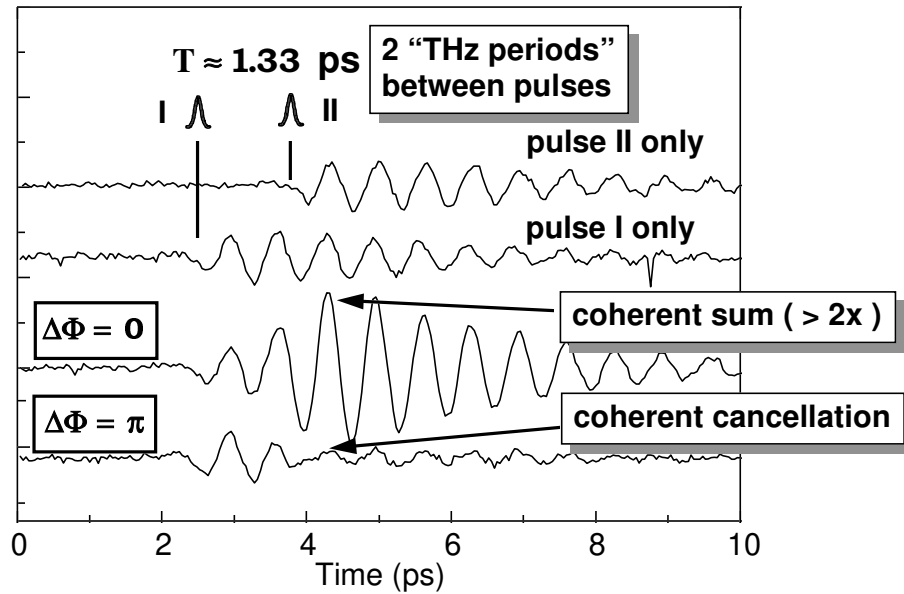
Fig. 17 Terahertz signals for excitation by two pulses separated by approximately 2 oscillation periods. The top two traces show the resulting signals for excitation by each of the two pulses separately. The bottom two traces show two cases for excitation with both pulses. One shows coherent addition of the two induced oscillations, the other shows coherent cancellation. Note that the difference between these two cases is only in the difference in the relative *optical* phase of the pulses.

   In such an experiment, we might imagine that the first pulses would set some charge oscillating, and the second pulse, being of essentially the same amplitude, would set up about the same amount again; given the carefully chosen time separation between the pulses, the second oscillation and the first would add, and we would get twice as much charge oscillating, and hence twice as much field generated. This is clearly not the case, as can be seen from the results. A key error in such an analysis is that we must add the wavefunctions first, then deduce the resulting observable. This has two kinds of consequences. First of all, if we indeed do manage to add the wavefunction created by the second pulse to the approximately equal oscillating wavefunction left over from the first pulse, we may indeed double the wavefunction amplitude that is oscillating; but the resulting terahertz current or polarization is proportional to the amount of charge oscillating, and the amount of charge oscillating is proportional to the *square* of the amplitude of the wavefunction. Hence the resulting terahertz electric field could actually *quadruple*, not merely double. This kind of effect is seen in the third trace (from the top) of Fig. 17.   The second consequence results because we must add the wavefunctions is that we must add the complete wavefunctions, not merely the envelopes. We must remember that the actual wavefunction of an electron in a quantum well is not really just the slowly-varying envelope we have been discussing. The slowly varying envelope is just the modulation envelope multiplying the unit cell wavefunctions. If we change the optical phase of a pulse by half a cycle, we will change the phase of oscillation of the unit cell wavefunctions by half a cycle. This can mean that the second pulse, if it has the wrong optical phase, can actually completely cancel the wavefunction generated by the first pulse by coherent cancellation at the unit cell level. This phenomenon is illustrated in the fourth (bottom) trace of Fig. 17; note that in going from the

third to the fourth traces in Fig. 17, all that has changed is the relative *optical* phase between the two pulses - a timing change of only 1.4 fs!

The experiment discussed here is only an illustration of the many quantum mechanical effects that can be explored optically in quantum wells. Further details on this and other current work can be found in the references (Roskos et al. 1992) (Brener et al. 1993) (Nuss et al. 1994) (Brener et al. 1994).

7. Conclusions

The optical properties of quantum wells near to the optical band-gap energy have proved to be a fascinating laboratory for studying many novel physical mechanisms. In addition, several novel and practical devices have resulted that offer significantly new opportunities for optoelectronic systems. We can expect continued evolution of physics, devices, and novel information processing systems in the years to come.

Further Reading

For an introductory summary of quantum well optical physics and devices, see Miller (1990a).
For a longer treatment of the physics, see Miller et al. (1988) and Chemla et al. (1988).
For an extensive discussion of quantum well optical physics see Schmitt-Rink et al. (1989).
For an extended discussion of band structure and states in quantum wells, see Bastard (1988).
For extended treatments of quantum well optoelectronic devices see Miller (1990b), Miller (1990c), and Lentine and Miller (1993).

References

Bastard G, 1988, Wave mechanics applied to semiconductor heterostructures (Les Editions de Physique, Les Ulis, France).

Brener I, Planken P C M, Nuss M C, Pfeiffer L, Leaird D E, and Weiner A M, 1993, Repetive excitation of charge oscillations in semiconductor heterostructures, Appl. Phys. Lett. Vol. 63 2213.

Brener I, Planken P C M, Nuss M C, Luo M S C, Chuang S L, Pfeiffer L, Leaird D E, and Weiner A M, 1994, Coherent control of terahertz emission and carrier populations in semiconductor heterostructures, 1994, J. Opt. Soc. Am. B (special issue on "Terahertz electromagnetic pulse generation, physics and applications"), to be published, Dec. 1994.

Burt M G, 1992, The justification for applying the effective-mass approximation to microstructures, J. Phys: Condens. Matter Vol. **4** 6651

Chemla D S, Miller D A B, Smith P W, Gossard A C, and Wiegmann W, 1984, Room temperature excitonic nonlinear absorption and refraction in GaAs/AlGaAs multiple quantum well structures, IEEE J. Quantum Electron. Vol. **20** 265.

Chemla D S, Schmitt-Rink S, and Miller D A B, 1988, Nonlinear Optical Properties of Semiconductor Quantum Wells, in Optical Nonlinearities and Instabilities in Semiconductors ed Haug H (Academic Press, Boston).

Chen Y K, Wu M C, Tanbun-Ek T, Logan R A, and Chin M A, 1991, Subpicosecond monolithic colliding-pulse mode-locked multiple quantum well lasers, Appl. Phys. Lett. Vol. **58** 1253.

Cho A Y, 1991, Advances in molecular beam epitaxy (MBE) Journal of Crystal Growth Vol. **111** 1.

D'Asaro L A, Chirovsky L M F, Laskowski E J, Pei S S, Woodward T K, Lentine A L, Leibenguth R E, Focht J W, Freund J M, Guth G G, and Smith L E, 1993, Batch fabrication and operation of GaAs-AlGaAs field-effect transistor-self-electrooptic effect device (FET-SEED) smart pixel arrays, IEEE J. Quantum Electron. Vol. **29** 670.

de Souza E A, Carraresi L, Boyd G D, and Miller D A B, 1993, Analog differential self-linearized quantum-well self-electro-optic-effect modulator, Optics Lett. Vol. **18** 974.

Furuya K, and Miyamoto Y, 1990, GaInAsP/InP organometallic vapor phase epitaxy for research and fabrication of devices, Int. J. High Speed Electronics Vol. **1** 347.

Goossen K W, Boyd G D, Cunningham J E, Jan W Y, Miller D A B, Chemla D S, and Lum R M, 1989, GaAs-AlGaAs multiquantum well reflection modulators grown on GaAs and silicon substrates, IEEE Photonics Tech. Lett. Vol. **1** 304.

Goossen K W, Cunningham J E, and Jan W Y, 1993, IEEE Photonics Tech. Lett. Vol. 5 776.

Keller U, 't Hooft G W, Knox W H, and Cunningham J E, 1991, Femtosecond pulses from a continuously self-starting passively mode-locked Ti:sapphire laser, {\itOptics Lett Vol. **16** 1022.

Lentine A L, Hinton H S, Miller D A B, Henry J E, Cunningham J E, and Chirovsky L M F, 1989, Symmetric self-electrooptic effect device: optical set-reset latch, differential logic gate, and differential modulator/detector, IEEE J. Quantum Electron. Vol. **25** 1928.

Lentine A L, McCormick F B, Cloonan T J, Sasian J M, Morrison R L, Beckman M G, Walker S L, Wojcik M J, Hinterlong S J, Crisci R J, Novotny R A, and Hinton H S, 1993, A five stage free-space switching network using arrays of FET-SEED switching nodes, Conference on Lasers and Electrooptics, May 2-7, 1993, Baltimore, Maryland Postdeadline Paper CPD24 (Optical Society of America)

Lentine A L, and Miller D A B, 1993, Evolution of the SEED technology: bistable logic gates to optoelectronic smart pixels, IEEE J. Quantum Electron. Vol. 29 655.

Miller D A B, Chemla D S, Damen T C, Gossard A C, Wiegmann W, Wood T H, and Burrus C A, 1985a, Electric field dependence of optical absorption near the bandgap of quantum well structures, Phys. Rev. B Vol. **32** 1043.

Miller D A B, Chemla D S, Damen T C, Wood T H, Burrus C A, Gossard A C, and Wiegmann W, 1985b, The quantum well self-electrooptic effect device: optoelectronic bistability and oscillation, and self linearized modulation, IEEE J. Quantum Electron. Vol. **QE-21** 1462.

Miller D A B, J. S. Weiner, and Chemla D S, 1986, Electric-field dependence of linear optical properties of quantum well structures: waveguide electroabsorption and sum rules, IEEE J. Quantum Electron. Vol. **QE-22** 1816.

Miller D A B, Chemla D S, and Schmitt-Rink S, 1988, Electric Field Dependence of Optical Properties of Semiconductor Quantum Wells: Physics and Applications, in Optical Nonlinearities and Instabilities in Semiconductors ed Haug H (Academic Press, Boston).

Miller D A B, 1989, Optics for low-energy communication inside digital processors: quantum detectors, sources, and modulators as efficient impedance converters, Optics Lett. Vol. **14** 146

Miller D A B, Feuer M D, Chang T Y, Shunk S C, Henry J E, Burrows D J, and Chemla D S, 1989, Field-effect transistor self-electrooptic effect device: integrated photodiode, quantum well modulator and transistor, IEEE Phot. Tech. Lett. Vol. **1** 61.

Miller D A B, 1990a, Optoelectronic applications of quantum wells, Optics and Photonics News Vol. 1, No. 2 (February 1990) 7.

Miller D A B, 1990b, Quantum Well Optoelectronic Switching Devices, Int. J. of High Speed Electronics Vol. 1 19.

Miller D A B, 1990c, Quantum-well self-electrooptic effect devices, Optical and Quantum Electron. Vol. **22** S61.

Miller D A B, 1993, "Novel analog self-electrooptic-effect devices", IEEE J. Quantum Electron. Vol. 29 655.

Nuss M C, Planken P C M, Brener I, Roskos H G, Luo M S C, and Chuang S L, 1994, Terahertz electromagnetic radiation from quantum wells, Appl. Phys. B Vol. 58 249.

Roskos H G, Nuss M C, Shah J, Leo K, Miller D A B, Fox A M, Schmitt-Rink S, and Köhler K, 1992, Coherent submillimeter-wave emission from charge oscillations in a double-well potential, Phys. Rev. Lett. Vol. 68 2216.

Schmitt-Rink S, Chemla D S, and Miller D A B, 1985, Theory of transient excitonic optical nonlinearities in semiconductor quantum-well structures, Phys. Rev. B Vol. **32** 6601

Schmitt-Rink S, Chemla D S, and Miller D A B, 1989, Linear and nonlinear optical properties of semiconductor quantum wells, Advances in Physics Vol. 38 89.

Smith P W, Silberberg Y, and Miller D A B, 1985, Mode locking of semiconductor diode lasers using saturable excitonic nonlinearities, J. Opt. Soc. Am. **B Vol. 2** 1228.

Tsang W T, 1990, Progress in chemical beam epitaxy, J. Crystal Growth Vol. **105** 1.

Weisbuch C, 1987, Fundamental properties of III-V semiconductor two-dimensional quantized structures: the basis for optical and electronic device applications, in Semiconductors and Semimetals Vol. 24, ed Dingle R (Academic Press, New York) 1.